

Integro-difference equations for interacting species and the Neolithic transition

J Fort, J Pérez-Losada, J J Suñol, L Escoda and J M Massaneda

Departament de Física, Universitat de Girona, 17071 Girona, Catalonia, Spain

E-mail: joaquim.fort@udg.edu

New Journal of Physics **10** (2008) 043045 (18pp)

Received 15 November 2007

Published 24 April 2008

Online at <http://www.njp.org/>

doi:10.1088/1367-2630/10/4/043045

Abstract. We introduce a set of sequential integro-difference equations to analyze the dynamics of two interacting species. Firstly, we derive the speed of the fronts when a species invades a space previously occupied by a second species, and check its validity by means of numerical random-walk simulations. As an example, we consider the Neolithic transition: the predictions of the model are consistent with the archaeological data for the front speed, provided that the interaction parameter is low enough. Secondly, an equation for the coexistence time between the invasive and the invaded populations is obtained for the first time. It agrees well with the simulations, is consistent with observations of the Neolithic transition, and makes it possible to estimate the value of the interaction parameter between the incoming and the indigenous populations.

Contents

1. Introduction	2
2. Evolution equations	3
2.1. Non-sequential models	3
2.2. Sequential model	5
3. Front speeds from CSRW	7
3.1. Integro-difference model	7
3.2. Sequential reaction-diffusion (SRD) approximation	9
4. Random walks on lattices	10
4.1. Numerical simulations	10
4.2. Upper and lower bounds on the CSRW speed	11
5. The coexistence time	13
6. Concluding remarks	16
Acknowledgments	17
References	17

1. Introduction

Interaction effects between several species lead to important changes in the dynamics of physical, chemical and biophysical systems [1, 2]. For example, the Neolithic transition is an important historical process in which an incoming farming population (Neolithic humans) invaded an area occupied by an indigenous population of hunter–gatherers (Paleolithic humans) [2]–[4]. Besides the Neolithic transition in Europe, reaction–dispersion models have been recently applied to other important processes in human history, such as the postglacial recolonization of Europe [5], the initial colonization of America [6], and the colonization of the US in the XIX century [7]. Such reaction–dispersal models are also important in many other systems of biophysical interest, such as forest range expansions [8], the spread of virus infections [9], tumor growth [10], etc.

In this paper, we consider some well-known reaction–dispersal models for interacting species (section 2.1) and modify them in order to take into account that in the case of human populations, children need to spend some time with their parents until they can survive on their own (section 2.2). We derive the corresponding speed of the invasion front analytically (section 3) and test the result using random-walk numerical simulations (section 4). The predicted front speed is consistent with that implied by archaeological observations of the Neolithic transition in Europe. Finally, we derive what we believe is the first analytical equation for the coexistence time between an invasive and an invaded population driven to extinction (section 5). It makes it possible to estimate the interaction parameter between the two populations (this parameter, in turn, has an effect on the front speed). The invading Neolithic and the indigenous Paleolithic peoples interact, and the latter become extinct. The coexistence time between the two can be measured from archeological data [11], so this gives a way to estimate the interaction parameter from observations (independent of the front speed). Moreover, the interaction parameter is known to play an important role in the geographical distribution of genes [11], so it is indeed important to estimate it from measurable data. This is now possible

via the equation for the coexistence time, which is derived and tested via numerical simulations in section 5. As in previous work [4, 12, 13], we shall here consider a two-dimensional (2D) space, so that we can apply our results to population range expansions on the Earth's surface.

2. Evolution equations

The models in this section may be called continuous-space random walks (CSRW), because they describe population density dynamics arising from random walks of individuals moving on a continuous surface. In contrast, numerical simulations (section 4) can only compute population densities on a finite number of points, so they necessarily simulate population dynamics on discrete surfaces (or spaces).

2.1. Non-sequential models

Let $p_N(\vec{r}, t)$ stand for the population number density of the Neolithic population, per unit area centered at position $\vec{r} \equiv (x, y)$ and time t . The dispersal kernel $\phi_N(\vec{\Delta})$ is the probability per unit area that an individual who was at $(\vec{r} + \vec{\Delta}, t) \equiv (x + \Delta_x, y + \Delta_y, t)$ jumps to $(\vec{r}, t + T)$. Here, T is the time interval between two subsequent jumps (according to anthropological data, $T = 1$ generation $\simeq 32$ years [13]¹). Let $R_N[p_N(x, y, t)]$ stand for the new individuals born (due to biological reproduction) during the time interval T (per unit area centered at \vec{r}). The evolution equation is typically written down as follows [4]:

$$p_N(\vec{r}, t + T) - p_N(\vec{r}, t) = T_N \left[p_N(\vec{r} + \vec{\Delta}, t) \phi_N(\vec{\Delta}) \right] - p_N(\vec{r}, t) + R_N [p_N(\vec{r}, t)], \quad (1)$$

where the population transport (or dispersal) operator is defined as

$$T_N \left[p_N(\vec{r} + \vec{\Delta}, t) \phi_N(\vec{\Delta}) \right] \equiv \int_{-\infty}^{+\infty} \int_{-\infty}^{+\infty} p_N(x + \Delta_x, y + \Delta_y, t) \phi_N(\Delta_x, \Delta_y) d\Delta_x d\Delta_y.$$

The first- and second-terms in the right-hand side (rhs) of equation (1) correspond the incoming minus outgoing individuals, and the last term $R_N[p_N(\vec{r}, t)]$ to net reproduction (births minus deaths per generation).

If there is a second species with number density $p_P(\vec{r}, t)$ (e.g. Paleolithic humans), an interaction term $\pm I[p_N(\vec{r}, t), p_P(\vec{r}, t)]$ is added to the previous equation,

$$p_N(\vec{r}, t + T) - p_N(\vec{r}, t) = T_N \left[p_N(\vec{r} + \vec{\Delta}, t) \phi_N(\vec{\Delta}) \right] - p_N(\vec{r}, t) + R_N [p_N(\vec{r}, t)] \pm I [p_N(\vec{r}, t), p_P(\vec{r}, t)] \quad (2)$$

and an analogous equation is written for the second species,

$$p_P(\vec{r}, t + T) - p_P(\vec{r}, t) = T_P \left[p_P(\vec{r} + \vec{\Delta}, t) \phi_P(\vec{\Delta}) \right] - p_P(\vec{r}, t) + R_P [p_P(\vec{r}, t)] - I [p_N(\vec{r}, t), p_P(\vec{r}, t)], \quad (3)$$

¹ For the estimation $T = 32$ yr of the generation time, see note 24 in [13].

where

$$T_P \left[p_P(\vec{r} + \vec{\Delta}, t) \phi_P(\vec{\Delta}) \right] \equiv \int_{-\infty}^{+\infty} \int_{-\infty}^{+\infty} p_P(x + \Delta_x, y + \Delta_y, t) \phi_P(\Delta_x, \Delta_y) d\Delta_x d\Delta_y.$$

Two situations can be considered: (i) the so-called competition case corresponds to the negative sign in equation (2), so that the interaction leads to a decrease in the number densities of both species. (ii) The so-called predator–prey case corresponds to the positive sign in equation (2), so that the interaction leads to an increase in the number density of species N and a decrease in the species P. We shall consider the latter case in the present paper, because in the Neolithic transition the interaction between the two populations (invading Neolithic farmers N and indigenous Paleolithic hunter–gatherers P) leads to an increase in the number density of N and a decrease of P. This may be due to a variety of possible causes (e.g. acculturation, interbreeding, etc [2]) but the important point is that observations of hunter–gatherers interacting with farmers always show an increase of farmers (N) (together, of course, with the same decrease of hunter–gatherers (P)) [2, 14]. Thus, the positive sign in equation (2) is appropriate for our case.

As in [15], we shall assume reproduction proportional to the population density, but bounded by a maximum value $p_{\max i}$ (due to the environmental limitations),

$$R_i[p_i(\vec{r}, t)] = \begin{cases} (R_{0i} - 1) p_i(\vec{r}, t), & \text{if } p_i < p_{\max i}, \\ 0, & \text{if } p_i \geq p_{\max i}, \end{cases} \quad (4)$$

where R_{0i} is called the net reproductive rate (or fecundity) per generation of the population i ($i = N$ and P), and $p_{\max i}$ is its saturation density [15]. As usual, we assume $R_{0i} > 1$ (otherwise the species i would become extinct) [16]. Let us mention that a logistic form for $R_i[p_i(\vec{r}, t)]$ is not appropriate for finite-difference models, because it yields negative population densities (see [17] for non-spatial models, and [15] for spatial models and a comparison of possible forms for $R_i[p_i(\vec{r}, t)]$).

We may note that, by Taylor expanding up to second order in space, assuming an isotropic kernel (i.e. that $\phi(\Delta_x, \Delta_y)$ depends only on $\Delta = \sqrt{\Delta_x^2 + \Delta_y^2}$), the former two equations become (for $p_i < p_{\max i}$)

$$p_N(\vec{r}, t + T) = D_N \left(\frac{\partial^2 p_N}{\partial x^2} + \frac{\partial^2 p_N}{\partial y^2} \right) + R_{0N} p_N(\vec{r}, t) + I [p_N(\vec{r}, t), p_P(\vec{r}, t)], \quad (5)$$

$$p_P(\vec{r}, t + T) = D_P \left(\frac{\partial^2 p_P}{\partial x^2} + \frac{\partial^2 p_P}{\partial y^2} \right) + R_{0P} p_P(\vec{r}, t) - I [p_N(\vec{r}, t), p_P(\vec{r}, t)], \quad (6)$$

where we have introduced the diffusion coefficients of the two species

$$D_i = \frac{1}{4T} \int_{-\infty}^{+\infty} \int_{-\infty}^{+\infty} \phi_i(\Delta) \Delta^2 d\Delta_x d\Delta_y \equiv \frac{\langle \Delta^2 \rangle_i}{4T}. \quad (7)$$

Let us mention that one can also perform Taylor expansions in time and obtain space-dependent Lotka–Volterra equations up to first order [17], hyperbolic equations up to second order [18], etc.

As usual [1, 17, 18], we assume that the interaction term is proportional to both population number densities (so that the interaction vanishes if one population (or both) is absent), but bounded so as to avoid negative values of $p_P(\vec{r}, t + T)$ in equation (6),

$$I [p_N(\vec{r}, t), p_P(\vec{r}, t)] = \begin{cases} \Gamma p_N(\vec{r}, t) p_P(\vec{r}, t), & \text{if } p_N < \frac{R_{0P}}{\Gamma}, \\ 0, & \text{if } p_N \geq \frac{R_{0P}}{\Gamma}. \end{cases} \quad (8)$$

The second line is included to avoid negative population densities, which have no physical meaning (it is thus similar to the second line in equation (4), which is included to avoid population densities above saturation, because they have no biological meaning). Nonlinear terms could be added to the first line in equation (8), but the parameter values would be very difficult (or even impossible) to estimate from the data available (and the speed of fronts would be the same). Thus, we finally arrive at the evolution equations (for $p_i < p_{\max i}$ and $p_N < \frac{R_{0P}}{\Gamma}$)

$$p_N(\vec{r}, t + T) = T_N \left[p_N(\vec{r} + \vec{\Delta}, t) \phi_N(\vec{\Delta}) \right] + (R_{0N} - 1) p_N(\vec{r}, t) + \Gamma p_N(\vec{r}, t) p_P(\vec{r}, t), \quad (9)$$

$$p_P(\vec{r}, t + T) = T_P \left[p_P(\vec{r} + \vec{\Delta}, t) \phi_P(\vec{\Delta}) \right] + (R_{0P} - 1) p_P(\vec{r}, t) - \Gamma p_N(\vec{r}, t) p_P(\vec{r}, t). \quad (10)$$

According to anthropological data, the generation times of pre-industrial farmers and hunter-gatherers are almost the same [5]. Therefore, we use a single parameter T for both populations because we expect that substantially more complicated models and simulations would lead to essentially the same results.

2.2. Sequential model

Models arising from equations, such as (9) and (10) have been widely considered in the literature [17]. They are very useful for non-living systems, e.g. molecules of several chemical species. They are also appropriate to some biological species. But, recently it has been noted that equations of this form have an important limitation if applied to human populations [7, 15]. It is thus very important to explain clearly this crucial point here. For humans, it is more realistic to replace the set of equations (9) and (10) by the following one:

$$p_N(\vec{r}, t + T) = T_N \left[p_N(\vec{r} + \vec{\Delta}, t) \phi_N(\vec{\Delta}) \right] + (R_{0N} - 1) T_N \left[p_N(\vec{r} + \vec{\Delta}, t) \phi_N(\vec{\Delta}) \right] + \Gamma \int_{-\infty}^{+\infty} \int_{-\infty}^{+\infty} p_N(\vec{r} + \vec{\Delta}, t) p_P(\vec{r} + \vec{\Delta}, t) \phi_N(\vec{\Delta}) d\Delta_x d\Delta_y, \quad (11)$$

$$p_P(\vec{r}, t + T) = T_P \left[p_P(\vec{r} + \vec{\Delta}, t) \phi_P(\vec{\Delta}) \right] + (R_{0P} - 1) T_P \left[p_P(\vec{r} + \vec{\Delta}, t) \phi_P(\vec{\Delta}) \right] - \Gamma \int_{-\infty}^{+\infty} \int_{-\infty}^{+\infty} p_N(\vec{r} + \vec{\Delta}, t) p_P(\vec{r} + \vec{\Delta}, t) \phi_P(\vec{\Delta}) d\Delta_x d\Delta_y. \quad (12)$$

In order to see, why equations (11) and (12) are more appropriate for humans than equations (9) and (10), we represent the model given by equations (9) and (10) in figure 1(a) and

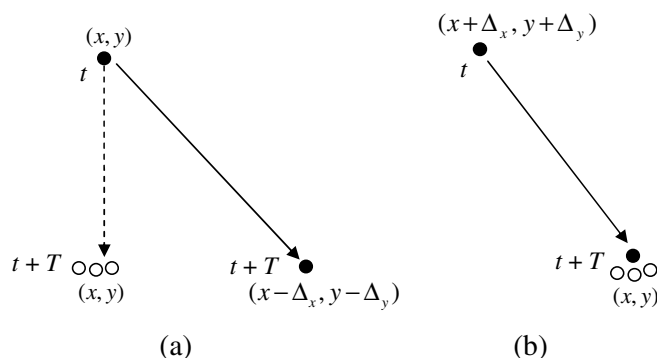


Figure 1. A filled circle represents a couple of parents (a father and a mother) and each empty circle stands for one of their sons or daughters. Reproduction is represented by the dashed arrow, migration by the continuous arrow. (a) Non-sequential model (section 2.1) and (b) Sequential model (section 2.2). This one is more appropriate for humans than model (a), because in model (a) parents migrate away from their children.

that given by equations (11) and (12) in figure 1(b). The first term in the rhs of equations (9) and (10) is the same as in equations (11) and (12). It corresponds to population dispersal or migration (continuous arrows in figure 1). However, the second term in the rhs (population reproduction) is different. According to this term in equations (9) and (10), children are born at $\vec{r} \equiv (x, y)$ (dashed arrow in figure 1(a)), so parents leave their newborn children alone (figure 1(a)). This may be realistic for some biological species (e.g. fish), but not for humans. In contrast, the second term in the rhs of equations (11) and (12) is an integral term, so in this model migrating parents live with their newborn children at their final location (figure 1(b)). This is realistic for humans². Therefore, as in [7, 15], we shall consider the model given by equations (11) and (12) (however, in [7, 15] a single population was considered, so equation (12) was not applied and the last term in equation (11) was absent).

Concerning the last term in equations (11) and (12), it leads to an increase in the population density of species N and a decrease in that of P due to their interaction (so we may represent this process as $N + P \rightarrow N$). As mentioned in the previous subsection, this interaction process $N + P \rightarrow N$ may be due to a variety of causes, such as interbreeding ($N + P \rightarrow N$) or acculturation ($N + P \rightarrow N + N \rightarrow N$). But in both cases, we think it is again more appropriate to use an integral over the dispersal kernel (just as in the second term in the rhs). The reason is that if we used the last terms in equations (9) and (10), then the final result (newborn N-individuals) would appear in the same location as that occupied a generation earlier by their parents (dashed arrow in figure 1(a)) and the latter would have migrated away from that location (continuous arrow in figure 1(a), i.e. first term in the rhs of equations (9) and (10)). In contrast, for the last terms in equations (11) and (12) parents do not migrate away from their newborn children (figure 1(b)).

² It may seem at first sight that the second term in the rhs of equations (11) and (12), namely $(R_{0N} - 1)(R_{0i} - 1) \int_{-\infty}^{+\infty} \int_{-\infty}^{+\infty} p_i(x + \Delta_x, y + \Delta_y, t) \phi_i(\Delta_x, \Delta_y) d\Delta_x d\Delta_y$, implies that children are born at the arrival location of their parents' migration. In fact, the same term holds if they are born at the initial location, namely $\int_{-\infty}^{+\infty} \int_{-\infty}^{+\infty} [(R_{0i} - 1) p_i(x + \Delta_x, y + \Delta_y, t)] \phi_i(\Delta_x, \Delta_y) d\Delta_x d\Delta_y$. The important point is that for these equations, parents do not migrate away from their children (see figure 1).

Theorems on the speed of front solutions for the first equation (11) without interaction ($p_P(\vec{r}, t) = 0$) have been derived previously [16], and the predicted speed has been compared to random-walk simulations on lattices [15] but again, only for the single-species case. In the next section, we tackle the general case of two species interacting with each other (i.e. we shall consider both equations (11) and (12) with $p_P(\vec{r}, t) \neq 0$).

3. Front speeds from CSRW

3.1. Integro-difference model

According to equations (11) and (12), our sequential model is finally given (for $p_i < p_{\max i}$ and $p_N < \frac{R_{0P}}{\Gamma}$) by

$$p_N(\vec{r}, t + T) = R_{0N} \int_{-\infty}^{+\infty} \int_{-\infty}^{+\infty} \left[1 + \gamma p_P(\vec{r} + \vec{\Delta}, t) \right] p_N(\vec{r} + \vec{\Delta}, t) \phi_N(\vec{\Delta}) d\Delta_x d\Delta_y, \quad (13)$$

$$p_P(\vec{r}, t + T) = R_{0P} \int_{-\infty}^{+\infty} \int_{-\infty}^{+\infty} \left[1 - \frac{\gamma R_{0N}}{R_{0P}} p_N(\vec{r} + \vec{\Delta}, t) \right] p_P(\vec{r} + \vec{\Delta}, t) \phi_P(\vec{\Delta}) d\Delta_x d\Delta_y, \quad (14)$$

where

$$\gamma \equiv \frac{\Gamma}{R_{0N}}. \quad (15)$$

As in [18], we assume that the invasion front of species N spreads in a region where the density of the indigenous species P is initially equal to its maximum possible value, $p_{\max P}$. This is appropriate for the Neolithic transition (i.e. the invasion of Neolithic farmers N into a space populated by indigenous Paleolithic hunter-gatherers P). Thus, in the leading edge of the invasion front we may write

$$p_N(\vec{r}, t) \simeq \varepsilon(\vec{r}, t) + O(2), \quad (16)$$

$$p_P(\vec{r}, t) \simeq p_{\max P} - \delta(\vec{r}, t) + O(2),$$

where $O(2)$ stands for second- and higher-order terms,

$$\varepsilon(\vec{r}, t) \ll p_{\max N} \quad (17)$$

and

$$\delta(\vec{r}, t) \ll p_{\max P}. \quad (18)$$

Therefore, up to first order we have for the interaction term

$$\gamma p_N(\vec{r}, t) p_P(\vec{r}, t) \simeq \gamma p_N(\vec{r}, t) p_{\max P} + O(2). \quad (19)$$

Such an approach was already applied in [18] to a different set of evolution equations. It is useful here because it reduces equation (13) to an evolution equation in which only the variable $p_N(\vec{r}, t) \equiv p_N(x, y, t)$ appears,

$$p_N(x, y, t + T) \simeq R_{0N} (1 + \gamma p_{\max P}) \int_{-\infty}^{+\infty} \int_{-\infty}^{+\infty} p_N(x + \Delta_x, y + \Delta_y, t) \phi_N(\Delta_x, \Delta_y) d\Delta_x d\Delta_y. \quad (20)$$

In the next section, we will check the validity of this approximation by means of numerical simulations of the two-species system (13) and (14).

The front speed of the invading species (farmers in the case of the Neolithic transition) can be found most easily by assuming that for $t \rightarrow \infty$ the front curvature is negligible (at scales much larger than that in which the front speed is measured), so that we can choose the x -axis parallel to the local velocity of the front [1]. Let $c \equiv |c_x|$ stand for the front speed ($c_y = 0$ in the local frame just introduced). We look for constant-shape solutions with the form $p_N = p_0 \exp[-\lambda(x - ct)]$ as $x - ct \rightarrow \infty$. Assuming an isotropic kernel $\phi(\Delta)$, we obtain from equation (20)

$$\exp[cT\lambda] = R_{0N}(1 + \gamma p_{\max P}) \int_0^\infty d\Delta \Delta \phi_N(\Delta) \int_0^{2\pi} d\theta \exp[-\lambda\Delta \cos \theta], \quad (21)$$

where $\theta \equiv \tan^{-1} \frac{\Delta_y}{\Delta_x}$. In order to perform the integrals, we need an expression for the kernel $\phi(\Delta)$. There are many possible choices of the kernel. Here, we are interested in the simplest possible kernel such that we can derive analytical formulae, so we simply assume that an individual will either remain at rest (with probability p_e , which is called the persistence in demography) or will move a distance r (with probability $1 - p_e$),

$$\phi_N(\Delta) = \phi_P(\Delta) = p_e \delta^{(2)}(\Delta) + (1 - p_e) \delta^{(2)}(\Delta - r) = p_e \frac{\delta^{(1)}(\Delta)}{2\pi \Delta} + (1 - p_e) \frac{\delta^{(1)}(\Delta - r)}{2\pi \Delta}, \quad (22)$$

where $\delta^{(2)}(\Delta - r)$ and $\delta^{(1)}(\Delta - r)$ are the 2D and 1D Dirac deltas centered at $\Delta = r$. In fact, there are some differences between the observed dispersal kernels of pre-industrial farmers ($\phi_N(\Delta)$) and hunter-gatherers ($\phi_P(\Delta)$), but these differences are small [5]. This may be surprising at first sight, given the fact that hunter-gatherers typically change their location many times during their lifetime [19, 20]. However, pre-industrial agriculturalists also have a high mobility because they practice slash-and-burn agriculture, using the land in a cyclic way and changing their location very often [21]. Indeed, typical dispersal distances observed for hunter-gatherers [22] are similar to those observed for pre-industrial farmers [5]. Therefore, we assume simply $\phi_N(\Delta) \simeq \phi_P(\Delta)$ in equation (22). This will avoid substantially more complicated simulations and analysis (which we do not expect to change the results appreciably).

After integrating equation (21), we assume as usual that the minimum speed is the one of the front [1] (in the next section, we will check this assumption by means of numerical simulations of the two-species system (13) and (14)). In this way, we obtain the front speed

$$c = \min_{\lambda > 0} \frac{\ln [R_{0N} (1 + \gamma p_{\max P}) (p_e + (1 - p_e) I_0(\lambda r))]}{T\lambda}, \quad (23)$$

where

$$I_0(\lambda r) \equiv \frac{1}{2\pi} \int_0^{2\pi} d\theta \exp[\lambda r \cos \theta] \quad (24)$$

is the modified Bessel function of the first kind and order zero. For the case in which a single species invades the habitat without interaction ($\gamma = 0$, or $p_{\max P} = 0$), we recover the single-species result discussed in the previous work [15].

In figure 2, we show the speed predicted by the CSRW (full line), equation (23), for parameter values appropriate for the Neolithic transition, as follows. The generation time is $T = 1$ generation = 32 yr [13]. The population number datasets for pre-industrial farmers that settled in previously unpopulated areas were collected by Birdsell [23], and the implied range for R_{0N} is 1.6–3.0 [15]. For the population persistence p_e (fraction of the population that does not move appreciably), we use the mean value $p_e = 0.38$ [15], which was estimated from the

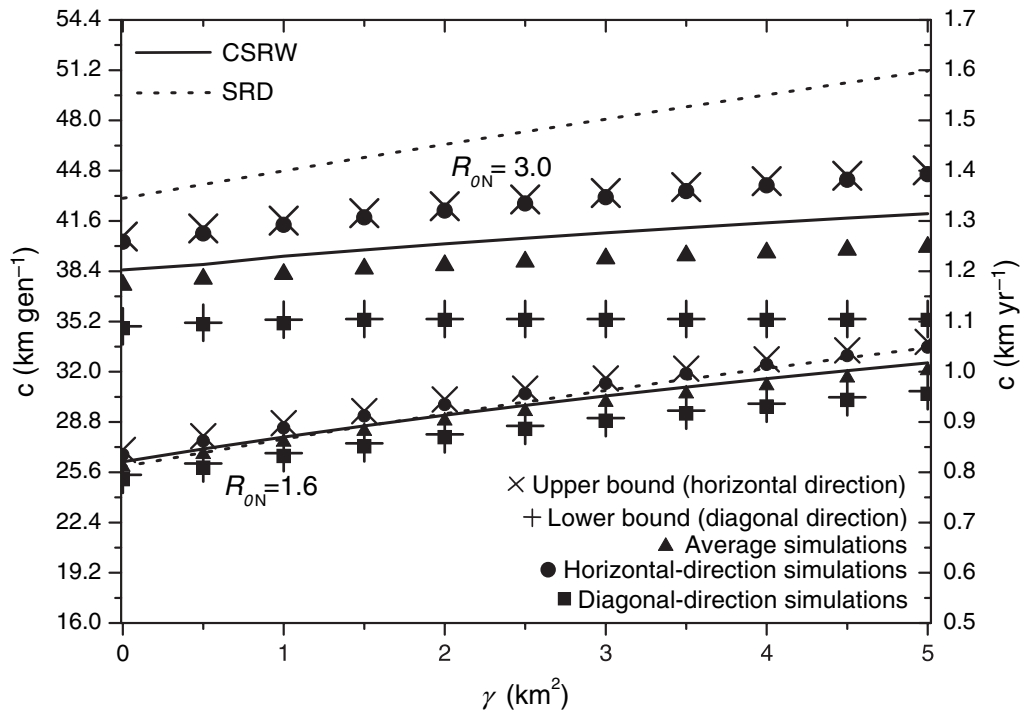


Figure 2. Predicted speeds as a function of the interaction parameter γ between the invading species N (farmers) and the indigenous species P (hunter-gatherers). They are seen to be consistent with the observed speed of the Neolithic transition in Europe, namely $0.6 \leq c \leq 1.3 \text{ km yr}^{-1}$ [24]. We have used $T = 32 \text{ yr}$, $R_{0P} = 1.8 \text{ gen}^{-1}$, $p_e = 0.38$, $p_{\max P} = 0.064 \text{ km}^{-2}$ and $p_{\max N} = 1.28 \text{ km}^{-2}$ (see sections 3.1 and 4.1).

mobility data in [21]. The value of r is estimated directly from those of the persistence and the mean-squared displacement³. For the maximum population density of hunter-gatherers, we use the same value as that applied by Currat and Excofier [11] in their genetic simulations of the Neolithic transition, namely $p_{\max P} = 0.064 \text{ hunter-gatherers km}^{-2}$.

In figure 2, the front speed predicted by the CSRW (full line), equation (23), is seen to increase with increasing values of the interaction parameter γ , as was expected intuitively because the higher its value, the more hunter-gatherers become farmers per generation (see, e.g. equation (20)).

3.2. Sequential reaction-diffusion (SRD) approximation

Equation (23) is not easy to apply in practice because it requires plotting a function and/or finding its minimum numerically for each set of parameter values. Therefore, here we derive a simpler approximation. The result will be also used to estimate the coexistence time (section 5). We approximate an equation (20) by using Taylor expansions in space and time up to second

³ We have computed the value of r such that the mean-squared displacement yields the observed value (namely 1544 km^2 [4]), i.e. $(1 - p_e)r^2 = \langle \Delta^2 \rangle = 1544 \text{ km}^2$. Using the mean value $p_e = 0.38$ (section 3.1), this yields $r \simeq 50 \text{ km}$.

order (assuming again an isotropic kernel),

$$p_N + T \frac{\partial p_N}{\partial t} + \frac{T^2}{2} \frac{\partial^2 p_N}{\partial t^2} \simeq R_{0N}(1 + \gamma p_{\max P}) p_N + R_{0N}(1 + \gamma p_{\max P}) DT \left(\frac{\partial^2 p_N}{\partial x^2} + \frac{\partial^2 p_N}{\partial y^2} \right), \quad (25)$$

where D is given by equation (7). The speed of this SRD equation may be derived, again, by assuming solutions with the form

$$p \simeq p_0 \exp[-\lambda(x - ct)] \quad (26)$$

with $\lambda > 0$. This yields

$$\lambda = \left(Tc + \left[(Tc)^2 - 4(R_{0N}(1 + \gamma p_{\max P}) - 1) \left(R_{0N}(1 + \gamma p_{\max P}) DT - \frac{T^2 c^2}{2} \right) \right]^{1/2} \right) \div (2R_{0N}(1 + \gamma p_{\max P}) DT - T^2 c^2). \quad (27)$$

Requiring λ to be real and assuming that the minimum speed is that of the front [1] we obtain the speed

$$c_{\text{SRD}} = \sqrt{\frac{2R_{0N}(1 + \gamma p_{\max P}) D}{T \left(1 + \frac{1}{2(R_{0N}(1 + \gamma p_{\max P}) - 1)} \right)}}. \quad (28)$$

In figure 2, we have also included this speed (dotted curves). It is seen to be a useful approximation, and it is much simpler to use than the exact result (23). Let us stress that we shall also use the approximate result (28) to estimate the coexistence time (section 5).

4. Random walks on lattices

4.1. Numerical simulations

In order to check the results of the previous section using numerical simulations, we consider a 2D lattice with 1000×1000 nodes. Initially, the invading population (N) is restricted to the central node of the grid (where $p_N(x, y, 0) = p_{\max N}$) and $p_N(x, y, 0) = 0$ elsewhere. For the indigenous population (P), initially $p_P(x, y, 0) = p_{\max P}$ everywhere except at the central node (which is occupied by the N-population, thus $p_P(x, y, 0) = 0$ at the central node).

At each time step (corresponding to $T = 1$ generation), we compute the new population number densities $p_N(x, y, t + T)$ and $p_P(x, y, t + T)$ at all nodes of the 2D lattice as follows:

(i) Firstly, according to the factor $[1 + \gamma p_P(x + \Delta_x, y + \Delta_y, t)]$ in equation (13), at every node (x, y) we add to the N-population density the term $\gamma p_N(x, y, t) p_P(x, y, t)$. And according to the factor $[1 - \frac{\gamma R_{0N}}{R_{0P}} p_N(x + \Delta_x, y + \Delta_y, t)]$ in equation (14), we subtract from the P-population the term $\frac{\gamma R_{0N}}{R_{0P}} p_N(x, y, t) p_P(x, y, t)$, unless a negative value for p_P is obtained. In the latter case, we set $p_P = 0$ (see the secondly line in equation (8); this corresponds to the local extinction of the invaded population).

(ii) Secondly, the dispersion of the population densities obtained in step (i) are performed using the kernel (22). Thus, a fraction p_e of each population (N and P) stays at the original node, and the remaining fraction is distributed equally among the nearest neighbors, i.e. a fraction $(1 - p_e)/4$ jumps a distance $\pm r$ along each horizontal or vertical direction. In the analytical model, this corresponds to the integrations in equations (13) and (14).

(iii) Finally, we compute the new N-population density due to reproduction at every node by multiplying $p_N(x, y, t)$ (obtained from step (ii)) by the factor R_{0N} (see, equation (13)), unless a value $p_N > p_{\max N}$ is obtained; in such a case we set $p_N = p_{\max N}$ (to avoid biologically unrealistic population densities over the saturation value implied by the environment, see the second line in equation (4)). Analogously, the new P-population density is computed as R_{0P} times the value of $p_P(x, y, t)$ from step (ii) (unless a value $p_P > p_{\max P}$ is obtained; in such a case we again set $p_P = p_{\max P}$).

For the net reproductive rate of hunter–gatherers, we use the characteristic value $R_{0P} = 1.8$.⁴ Saturation population densities for pre-industrial farmers and hunter–gatherers have been measured for several populations. In figure 2, we use the same values as those applied by Currat and Excofier [11] in their genetic simulations of the Neolithic transition, namely $p_{\max N} = 1.28 \text{ farmers km}^{-2}$ and $p_{\max P} = 0.064 \text{ hunter–gatherers km}^{-2}$.

We repeat this 3-step cycle many times, until we observe that the front speed is constant (this happens before 500 cycles or generations).

Along the horizontal/vertical directions of the lattice, the speed obtained from the simulations (circles in figure 2) is faster than that measured along the diagonal directions ($\pm 45^\circ$ relative to the horizontal axis) (squares). This is simply due to the fact that in our simulations, there are only jumps along the horizontal/vertical directions (otherwise the computer time would be much longer), so after two jumps the maximum distance moved in the diagonal direction ($r\sqrt{2}$) is lower than that in the horizontal/vertical direction ($2r$). The average of both speeds from the simulations (triangles in figure 2) agrees with the CSRW (full curves). Of course, we could try to attain better agreement by computing the simulated speeds along many other directions, but such additional tedious computations seem unnecessary because the validity of the analytical result is clear from figure 2 (full curves versus triangles). The small differences are not unexpected after all, because on a continuous surface jumps take place into all infinite points of a circle (CSRW model) but in simulations they necessarily take place into the nodes of a square (i.e. on a discrete surface). This also explains the asymptotic behavior of the diagonal simulations (squares) for $R_{0N} = 3.0$ in figure 2.⁵ We also check these simulation results analytically in the next subsection.

4.2. Upper and lower bounds on the CSRW speed

4.2.1. Upper bounds (horizontal/vertical direction). For a lattice in 2D space and the kernel (22), individuals can jump into point (x, y) from points $(x \pm r, y)$ and $(x, y \pm r)$. Therefore, in discrete space equation (20) is replaced by

$$p_N(x, y, t + T) = R_{0N}(1 + \gamma p_{\max P}) \{ p_e p_N(x, y, t) + (1 - p_e) \times \left[\frac{1}{4} p(x - r, y, t) + \frac{1}{4} p(x + r, y, t) + \frac{1}{4} p(x, y - r, t) + \frac{1}{4} p(x, y + r, t) \right] \}. \quad (29)$$

⁴ $R_{0P} = \exp[a_P T]$ (see note (26) in [15]) and we use the mean value $a_P = 0.022 \text{ yr}^{-1}$ from [5].

⁵ The fastest possible front speed along the horizontal or vertical directions of the square lattice will obviously be r/T (recall that r is the distance between the two nearest nodes, and T the time between the two successive jumps). This limit should be obtained for sufficiently high values of R_{0N} , so that the front propagation becomes diffusion-limited. Similarly, the fastest possible front speed along the diagonal directions of the square lattice will obviously be $r\sqrt{2}/(2T) \simeq 50 \text{ km}/(\sqrt{2} \cdot 32 \text{ yr}) = 1.1 \text{ km yr}^{-1}$, which agrees with the asymptotic behavior of the diagonal results (squares and + crosses) observed in figure 2 for $R_{0N} = 3.0$.

As in section 2, we look for solutions with the form $p = p_0 \exp[-\lambda(x - ct)]$ and assume that the minimum speed is the one of the front [1]. In this way, we obtain the speed

$$c = \min_{\lambda > 0} \frac{\ln \left[R_{0N}(1 + \gamma p_{\max P}) (p_e + (1 - p_e 2) / [\cosh(\lambda r) + 1]) \right]}{\lambda T}. \quad (30)$$

This equation has no analytical solution. However, for given values of R_0 , p_e , r , T and γ it is easy to find its minimum numerically. In this way, we obtain the crosses (\times) in figure 2. They agree perfectly with the horizontal/vertical-direction random-walk simulations, performed in the previous section (circles in figure 2).

4.2.2. *Lower bounds (diagonal direction).* Now, we choose X' and Y' forming 45° with the X - and Y -axes. Then, individuals jump into point (x', y') from points $(x' \pm \frac{r}{\sqrt{2}}, y' \pm \frac{r}{\sqrt{2}})$ so, instead of equation (29) we have

$$p_N(x', y', t + T) = R_{0N}(1 + \gamma p_{\max P}) \left\{ p_e p_N(x', y', t) + (1 - p_e) \times \left[\frac{1}{4} p_N \left(x' + \frac{r}{\sqrt{2}}, y' + \frac{r}{\sqrt{2}}, t \right) + \frac{1}{4} p_N \left(x' + \frac{r}{\sqrt{2}}, y' - \frac{r}{\sqrt{2}}, t \right) + \frac{1}{4} p_N \left(x' - \frac{r}{\sqrt{2}}, y' + \frac{r}{\sqrt{2}}, t \right) + \frac{1}{4} p_N \left(x' - \frac{r}{\sqrt{2}}, y' - \frac{r}{\sqrt{2}}, t \right) \right] \right\}, \quad (31)$$

which leads us, in the same way, to the speed

$$c = \min_{\lambda > 0} \frac{\ln \left[R_{0N}(1 + \gamma p_{\max P}) \left(p_e + (1 - p_e) \cosh \left(\lambda \frac{r}{\sqrt{2}} \right) \right) \right]}{\lambda T}, \quad (32)$$

instead of (30). This speed is shown as crosses (+) in figure 2. It agrees perfectly with the diagonal-direction simulations (squares in figure 2).

The agreement between the discrete-space analytical model (equations (30) and (32)) and the simulations (figure 2) confirms the validity of the lattice simulations in the previous subsection, and of equations (30) and (32) as upper and lower bounds on the exact (CSRW) speed.

Both the analytical results and the simulations (figure 2) are seen to be consistent with the observed speed of the Neolithic transition in Europe, namely $0.6 \leq c \leq 1.3 \text{ km yr}^{-1}$ [24], provided that the interaction parameter γ is low enough, e.g. $\gamma < 5 \text{ km}^2$ for $R_{0N} = 3.0$. Such a high value for R_{0N} is usually regarded as the highest possible net reproduction rate for pre-industrial agriculturalists, and it is considered reasonable for the Neolithic range expansions⁶. In principle, however, lower values could apply to regions less favorable for agriculture (e.g. $R_{0N} = 1.6$, which is the lowest value consistent with the population number series in [23], so we also include it in figure 2).

Finally, we stress that we have considered the so-called predator–prey case (positive sign in equation (2)) because we are here interested in the Neolithic transition, but the same methods above could be applied to the so-called competition case (negative sign in equation (2)) to derive the front speed. The competition case is relevant in many biological invasions, because in many

⁶ Using the relationship $a_N = (\ln R_{0N})/T$ (see note (26) in [15]) yields the estimations $a_N = 0.034 \text{ yr}^{-1}$ for $R_{0N} = 3.0$ and $a_N = 0.015 \text{ yr}^{-1}$ for $R_{0N} = 1.6$. This includes the range estimated from fits to differential-equation models in [4, 24], namely $0.029 \leq a_N \leq 0.035 \text{ yr}^{-1}$ or $2.53 \leq R_{0N} \leq 3.06$.

cases the invading population does not experience an increase in numbers due to its interaction with the indigenous population (e.g. for the gray and red squirrels in Britain [25]–[27]).

5. The coexistence time

The value of the parameter γ determines the strength of the interaction between the two species (or populations, in the case of the Neolithic transition). This parameter is important to predict the range expansion speed (figure 2). It is also of crucial importance in models of the geographic distribution of genes after a range expansion [11]. This can be understood intuitively as follows. For the limiting case of complete replacement without interaction ($\gamma = 0$) the genetic composition of the final population will obviously be Neolithic, not a mixture of both (Neolithic and Paleolithic) original gene pools. For higher interbreeding rates between the incoming (N) and pre-existing (P) populations (higher the value of γ), the local genetic composition of the population will vary more rapidly in space (near the origin of the population range expansion). Therefore, the value of γ affects the population genetics in addition to the front speed (figure 2). For both reasons, it is indeed interesting to find a way to estimate the value of γ from observations other than the front speed.

Intuitively, it is reasonable to expect that the coexistence time, i.e. that elapsed between the arrival of the invading population (N) and the extinction of the indigenous one (P), should be a way to determine the interaction parameter γ (and thus Γ) from observations. Indeed, for a stronger interaction (higher value of γ) the invading population (N) should reach its saturation value sooner, the indigenous one (P) should disappear more rapidly, and the coexistence time should be lower. Therefore, we expect the coexistence time to decrease with increasing values of the interaction parameter γ .

Although there are many papers on invasion front speeds, we are not aware of any equation for the coexistence time in the literature. To derive such an equation, we begin noting that the time rate of change of the invading population density at (x, y, t) can be estimated using equation (29) as

$$\frac{p_N(x, y, t+T) - p_N(x, y, t)}{T} = \frac{R_{0N}}{T} (1 + \gamma p_{\max P}) \left\{ p_e p_N(x, y, t) + \frac{1 - p_e}{4} [p(x-r, y, t) + p(x+r, y, t) + p(x, y-r, t) + p(x, y+r, t)] \right\} - \frac{p_N(x, y, t)}{T}. \quad (33)$$

For $p_N \simeq p_{\max N}/2$, we have $p_N(x-r, y, t) \simeq p_{\max N}$ (see figure 3(a))⁷. On the other hand, as in section 3 we assume that for $t \rightarrow \infty$ the front curvature is negligible so that we can choose the x -axis parallel to the local front speed and, in this frame, p_N depends only on x but not on y [1]. Therefore, $p(x, y-r, t) \simeq p(x, y+r, t) \simeq p(x, y, t) \simeq p_{\max N}/2$ and we obtain from equation (33)

$$s \equiv \frac{p_N(x, y, t+T) - p_{\max N}/2}{T} \simeq \frac{R_{0N}}{T} (1 + \gamma p_{\max P}) p_{\max N} \times \left(\frac{p_e}{2} + \frac{1 - p_e}{4} \left[2 + \frac{p(x+r, y, t)}{p_{\max N}} \right] \right) - \frac{p_{\max N}}{2T}. \quad (34)$$

⁷ Similarly, one could be tempted to approximate $p(x+r, y, t) \simeq 0$, but from figure 3(a) we note that this would be a rather strong approximation. In fact, instead of equation (41), it yields $t_c \simeq \max\{4T, 4T/(R_{0N}(1 + \gamma p_{\max P}) - 1)\}$, and this equation has a mean error of about 11% (relative to the simulations). So in the main text we derive a more accurate equation, without making this approximation.

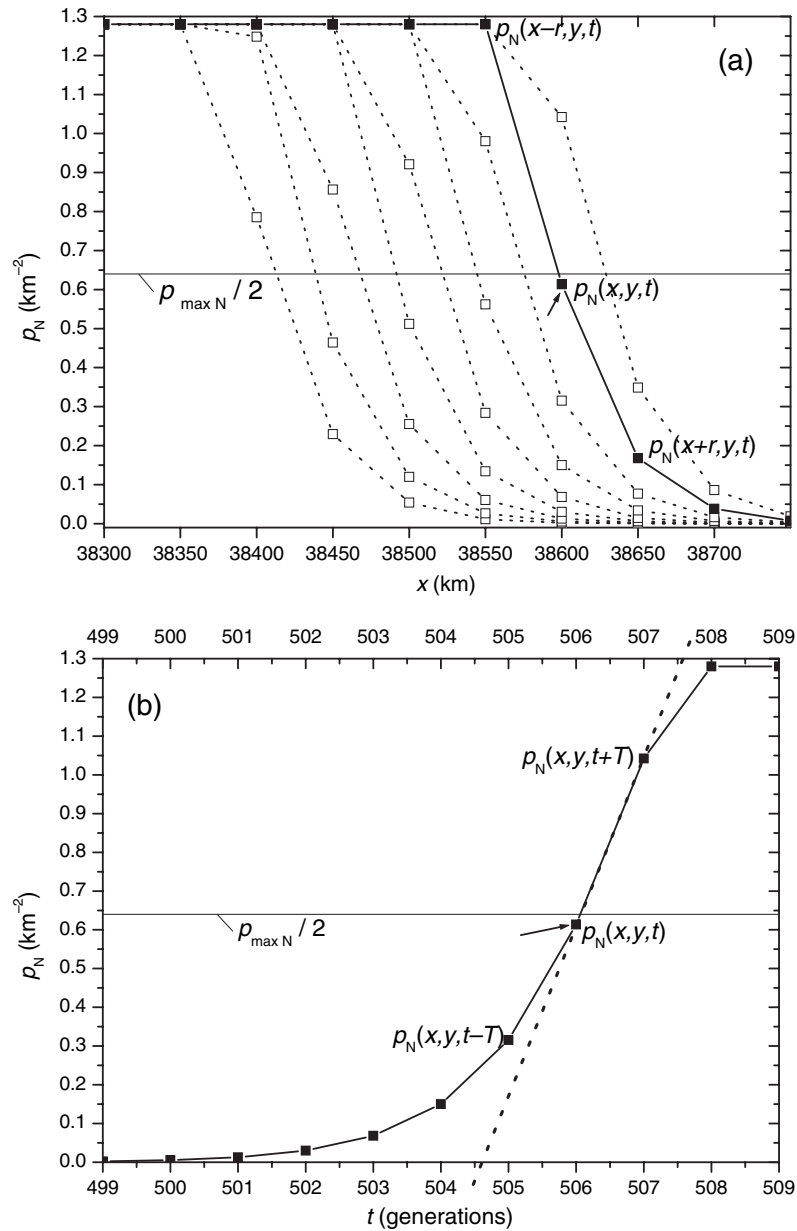


Figure 3. (a) Front profiles for $t = 499, 500, \dots, 507$ generations (from left to right). The full squares and line connecting them correspond to a front with a node such that $p_N(x, y, t) \simeq p_{\max N}/2$ (arrow), for which it is seen that $p_N(x - r, y, t) \simeq p_{\max N}$ but $p_N(x + r, y, t) \neq 0$. This is used to derive an equation (34). (b) Plot of the invading population density as a function of time at a given space point. The slope is estimated at the same space-time point as in (a) (arrow) and its corresponding straight line (dotted) implies a characteristic time of about $507.5 - 504.5 = 3$ generations. On the other hand, a reasonable estimation of the time needed by the population to saturate is about $508 - 502 = 6$ generations, i.e. about twice that implied by the slope. We have checked that the same happens for other parameter values. This yields equation (36). In these figures $R_{0N} = 1.6$, $\gamma = 0.1 \text{ km}^2$, and the rest of the parameter values are as in figure 2.

This gives the slope of the plot of p_N versus time at a given space point (x, y) for values of t such that $p_N \simeq p_{\max N}/2$ (see figure 3(b)). However, equation (34) will break down if the value of $p_N(x, y, t + T)$ implied by equation (33) is above saturation density, i.e. $p_N(x, y, t + T) > p_{\max N}$, because this is biologically impossible. Indeed, as shown by the second line in equation (4), reproduction stops at $p_{\max N}$, so in such an instance $p_N(x, y, t + T) = p_{\max N}$ and the slope at $p_N = p_{\max N}/2$ obviously reaches its maximum possible value, namely $s = (p_{\max N} - p_{\max N}/2)/T = p_{\max N}/(2T)$. Below we check this via numerical simulations. Therefore, in general equation (34) should be replaced by

$$s = \min \left\{ p_{\max N}/2T, \frac{R_{0N}}{T} (1 + \gamma p_{\max P}) p_{\max N} \left(\frac{p_e}{2} + \frac{1 - p_e}{4} \left[2 + \frac{p(x+r, y, t)}{p_{\max N}} \right] \right) - \frac{p_{\max N}}{2T} \right\}. \quad (35)$$

In order to derive an analytical result for the coexistence time, we estimate it as the time elapsed since the arrival of the invasive population (N) until it reaches its maximum value ($p_{\max N}$). From figure 3(b) and its caption, we see that a reasonable estimate of the coexistence time is given by

$$t_c \simeq 2t_{c\text{slope}} = 2 \frac{p_{\max N}}{s}, \quad (36)$$

where $t_{c\text{slope}}$ is the time estimated from the slope (see the dotted line in figure 3(b) and its caption; for that example $t_{c\text{slope}} \simeq 3$ generations and $t_c \simeq 6$ generations). Then, we may apply equation (35) and obtain

$$t_c \simeq \max \left\{ 4T, 2T \left/ \left[R_{0N}(1 + \gamma p_{\max P}) \left(\frac{p_e}{2} + \frac{1 - p_e}{4} \left[2 + \frac{p(x+r, y, t)}{p_{\max N}} \right] \right) - \frac{1}{2} \right] \right. \right\}, \quad (37)$$

but in order to obtain an equation for t_c in terms only of parameters appearing in the evolution equations, we still need a value for $p_N(x+r, y, t)$. An explicit estimation can be obtained by resorting to the SRD approximation, equations (26)–(28). Neglecting second-order terms for simplicity, it yields

$$\frac{p_{\max N}}{2} = p_N(x, y, t) \simeq p_0 \exp[-\lambda(x - ct)] \quad (38)$$

and

$$p_N(x+r, y, t) \simeq p_0 \exp[-\lambda(x+r - ct)], \quad (39)$$

with $\lambda \simeq \sqrt{\frac{R_{0N}-1}{R_{0N}DT}}$. Therefore,

$$p_N(x+r, y, t) \simeq \frac{p_{\max N}}{2} \exp \left[-r \sqrt{\frac{R_{0N}-1}{R_{0N}DT}} \right]. \quad (40)$$

Inserting this in equation (37), we finally obtain an equation for the coexistence time in terms only of the parameters appearing in the evolution equations, namely

$$t_c \simeq \max \left\{ 4T, 4T \left/ \left[R_{0N}(1 + \gamma p_{\max P}) \left(1 + \frac{1 - p_e}{4} \exp \left[-r \sqrt{\frac{R_{0N}-1}{R_{0N}DT}} \right] \right) - 1 \right] \right. \right\}. \quad (41)$$

In figure 4, we compare this equation to the values for the coexistence time obtained from the numerical simulations. The latter have been obtained by estimating the slope at $p_{\max N}/2$

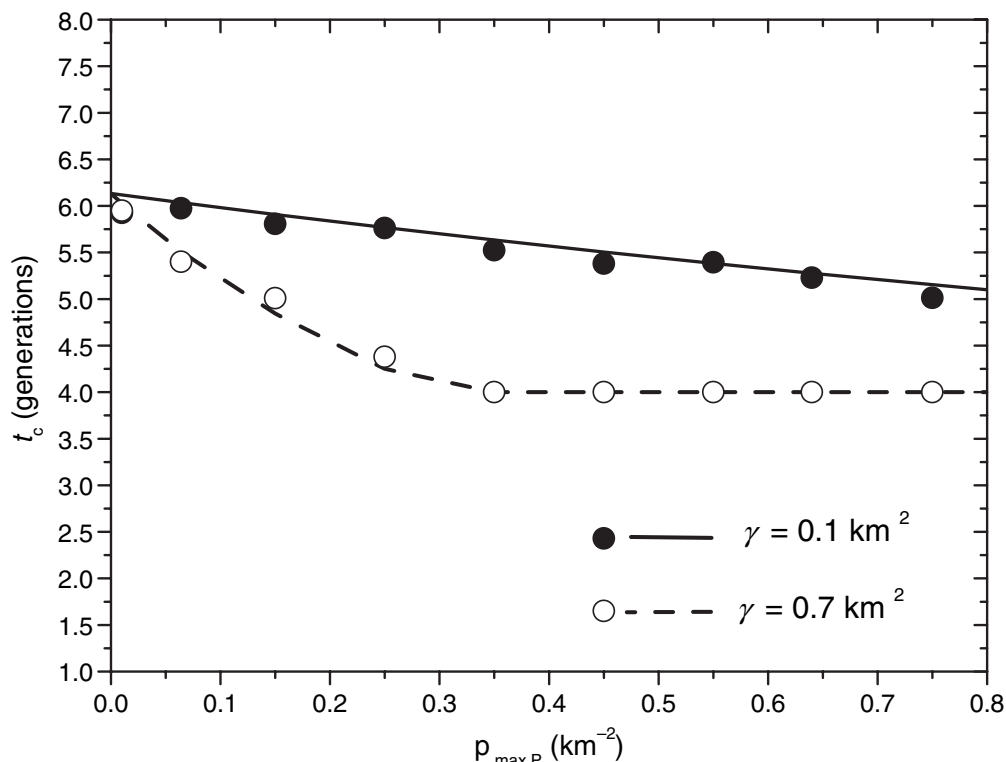


Figure 4. Comparison between the coexistence time predicted by equation (41) and observed in the simulations (circles). We have used $R_{\text{ON}} = 1.6$, and the remaining parameter values are the same as in figure 2.

from plots, such as figure 3(b) and using equation (36). There is good agreement between the analytical and the simulation results. This makes it possible to estimate the parameter γ if the coexistence time is known. In the Neolithic transition in Europe, according to archaeological observations, typical coexistence times are in the range 150–200 years [11], i.e. 4.7–6.3 generations, which is consistent with figure 4. In this figure, we plot the coexistence time as a function of the hunter–gatherer (i.e. Paleolithic) population density $p_{\max P}$, which is known to vary geographically depending on the availability of nutritional resources [2]. For example, for the value $p_{\max P} = 0.3 \text{ km}^{-2}$ figure 4 implies that a coexistence time of about 6 generations corresponds to $\gamma = 0.1 \text{ km}^2$ and a coexistence time of about 4 generations corresponds to $\gamma = 0.7 \text{ km}^2$. Interestingly, archaeological data imply different typical coexistence times in different regions [11], so our new analytical result (41) makes a non-uniform estimation of the value of γ possible from observations of the coexistence time. We would like to stress, however, that the result (41) is not limited to the Neolithic transition. It can be applied to all systems described by the predator–prey set of evolution equations (13) and (14).

6. Concluding remarks

Dispersal kernels have been applied to generalize reaction–diffusion equations in a variety of interesting situations. Besides the seminal results due to Weinberger, which were motivated by population genetics [16], dispersal kernels have been used in models of epidemic spread [28]–[30], biological invasions [31, 32], periodic wave trains in predator–prey

systems [33], accelerated invasions due to fat-tailed kernels [34], invasions constrained by interspecific competition [35], rapid plant migration [8], stage-structured populations [36, 37], invasions in 2D space [38, 39], etc. Here, we have presented an integro–difference model for interacting human populations which is more realistic than models based on differential equations [17, 18, 27], and used it: (i) to explain the speed of the Neolithic transition in Europe (figure 2); (ii) to derive an analytical equation for the coexistence time, equation (41), which is the first one to the best of our knowledge.

For stronger interactions between invading and invaded populations (higher value of Γ and thus γ), the invasion front spreads faster (equation (23) and figure 2), the coexistence time is shorter (equation (41) and figure 4), and the genetic cline will be steeper (section 5).

An interesting question that has not been analyzed previously in the literature is to what extent the observations available make it possible to determine some plausible range for the interaction parameter γ . This will in general depend on the geographical region. For example, a region where agriculture is very productive will likely correspond to a high value for the net reproductive rate of the farming (Neolithic) populations, e.g. $R_{0N} = 3.0$. Then figure 2 implies that $\gamma < 5 \text{ km}^2$ for the speed to fall into the observed range, $0.6 \leq c \leq 1.3 \text{ km yr}^{-1}$ [24] (see section 4 for a detailed discussion). In regions less suitable for agriculture, the value of R_{0N} will be lower. Then, the observed front speed ($0.6 \leq c \leq 1.3 \text{ km yr}^{-1}$) allows for a wider-range of γ (see figure 2 for $R_{0N} = 1.6$) but observations of the coexistence time t_c can be used to estimate the value of γ . For example, for $p_{\max P} = 0.3 \text{ km}^{-2}$ figure 4 implies that a coexistence time of about 6 generations corresponds to $\gamma = 0.1 \text{ km}^2$ and a coexistence time of about 4 generations corresponds to $\gamma = 0.7 \text{ km}^2$. These results are interesting on their own, because now, we have a clear set of equations and plausible parameter values for modeling the Neolithic transition. The new equation (41) for the coexistence time is also of interest in biological invasions and other systems described by the set (13) and (14). Additionally, our results are relevant also because of the crucial importance of the parameter γ in the modeling of population genetics arising from population range expansions [11]. Finally, this paper opens the way to regional analyses in which: (i) observed geographic differences in the coexistence times [11] could be used to estimate non-homogeneous values for the interaction parameter γ (figure 4) and therefore for the front speed (figure 2); (ii) regions less suitable for agriculture may correspond to lower values for R_{0N} and thus have a slower front speed (figure 2), which is consistent with the empirical observation that the Neolithic front slowed down as it approached colder regions in Northern Europe [40].

The results here reported could be extended to the case of anisotropic random walks, which may be essential in capturing the inhomogeneities inherent to the Neolithic and other population range expansions [3, 7].

Acknowledgments

Funded by the European Commission (grant NEST-28192-FEPRE), the MEC-FEDER (grant FIS-2006-12296-C02-02) and the Generalitat de Catalunya (grant SGR-2005-00087).

References

- [1] Fort J and Méndez V 2002 *Rep. Prog. Phys.* **65** 895
- [2] Ammerman A J and Cavalli-Sforza L L 1984 *The Neolithic Transition and the Genetics of Population in Europe* (Princeton: Princeton University Press)

- [3] Davison K, Dolukhanov P, Sarson G R and Shukurov A 2006 *J. Archaeol. Sci.* **33** 641
- [4] Fort J and Méndez V 1999 *Phys. Rev. Lett.* **82** 867
- [5] Fort J, Pujol T and Cavalli-Sforza L L 2004 *Camb. Archaeol. J.* **14** 53
- [6] Hamilton M J and Buchanan B 2007 *Proc. Natl Acad. Sci. USA* **104** 15625
- [7] Fort J and Pujol T 2007 *New J. Phys.* **9** 234
- [8] Clark J S 1998 *Am. Nat.* **152** 204
- [9] Fort J and Méndez V 2002 *Phys. Rev. Lett.* **89** 178101
- [10] Garner A L, Lau Y Y, L Jackson T L, Uhler M D, Jordan D W and Gilgenbach R M 2005 *J. Appl. Phys.* **98** 124701
- [11] Currat M and Excofier L 2005 *Proc. R. Soc. B* **272** 679
- [12] Fort J, Pérez J, Ubeda E and García J 2006 *Phys. Rev. E* **73** 021907
- [13] Fort J, Jana D and Humet J 2004 *Phys. Rev. E* **70** 031913
- [14] Cavalli-Sforza L L (ed) 1986 *African Pygmies* (Orlando: Academic)
- [15] Fort J, Pérez-Losada J and Isern N 2007 *Phys. Rev. E* **76** 031913
- [16] Weinberger H F 1978 *Nonlinear Partial Differential Equations and Applications* ed J Chadam (Berlin: Springer)
- [17] Murray J D 2002 *Mathematical Biology* 3rd edn, vol 2 (Berlin: Springer-Verlag)
- [18] Méndez V, Fort J and Farjas J 1999 *Phys. Rev. E* **60** 5231
- [19] Flood J 1976 *Tribes and Boundaries in Australia* ed N Peterson (Canberra: Australian Institute of Aboriginal Studies) pp 30–49
- [20] Turnbull C M 1986 *African Pygmies* ed L L Cavalli-Sforza (Orlando: Academic Press) pp 103–23
- [21] Stauder J 1971 *The Majangir: Ecology and Society of a Southwest Ethiopian People* (Cambridge: Cambridge University Press)
- [22] Hewlett B S, Van de Koppel J M H and Cavalli-Sforza L L 1986 *African Pygmies* ed L L Cavalli-Sforza (Orlando: Academic Press) pp 65–79
- [23] Birdsall J P 1957 *Cold Spring Harb. Symp. Quant. Biol.* **22** 47
- [24] Pinhasi R, Fort J and Ammerman A J 2005 *PLoS Biol.* **3** 2220–8
- [25] Okubo A, Maini P K, Williamson M H and Murray J D 1989 *Proc. R. Soc. Lond. B* **238** 113
- [26] Reynolds J C 1985 *J. Anim. Ecol.* **54** 149
- [27] Ortega-Cejas V, Fort J and Méndez V 2006 *Physica A* **366** 299
- [28] Diekmann O 1978 *J. Math. Biol.* **6** 109
- [29] Thieme H R 1979 *J. Math. Biol.* **8** 173
- [30] Schofield P 2002 *J. Theor. Biol.* **215** 121
- [31] van den Bosch F, Metz J A J and Diekmann O 1990 *J. Math. Biol.* **28** 529
- [32] van den Bosch F, Hengeveld R and Metz J A J 1991 *J. Biogeography* **19** 135
- [33] Kot M 1992 *J. Math. Biol.* **30** 413
- [34] Kot M, Lewis M A and van den Driessche P 1996 *Ecology* **77** 2027
- [35] Hart D R and Gardner R H 1997 *J. Math. Biol.* **35** 935
- [36] Neubert M G and Caswell H 2000 *Ecology* **81** 1613
- [37] Caswell H, Lensink R and Neubert M G 2003 *Ecology* **84** 1968
- [38] Lewis M A, Neubert M G, Caswell H, Clark J S and Shea K 2006 *Conceptual Ecology and Invasion Biology: Reciprocal Approaches to Nature* ed M Cadotte, S McMahon and T Fukami (Dordrecht: Kluwer)
- [39] Pielaat A, Lewis M A, Ieale S and de-Camino-Beck T 2006 *Ecol. Modelling* **190** 205
- [40] Ammerman A J 2003 *The Widening Harvest: The Neolithic Transition in Europe-Looking Back, Looking Forward* ed A J Ammerman and P Biagi (Boston: Archaeological Institute of America) pp 3–23